Femtotesla atomic magnetometry in a microfabricated vapor cell

W. Clark Griffith,[1,2,*] Svenja Knappe,[1,3] and John Kitching[1]

[1]*Time and Frequency Division, National Institute of Standards and Technology, 325 Broadway, Boulder, Colorado 80305, USA*
[2]*Currently with Los Alamos National Laboratory, Subatomic Physics Group (P-25), Los Alamos, New Mexico 87545, USA*
[3]*Also with University of Colorado, Boulder, Colorado 80309, USA*
[*]*wclarkg@gmail.com*
http://tf.nist.gov/timefreq/ofm/smallclock/Welcome.html

Abstract: We describe an optically pumped ^{87}Rb magnetometer with 5 fT/Hz$^{1/2}$ sensitivity when operated in the spin-exchange relaxation free (SERF) regime. The magnetometer uses a microfabricated vapor cell consisting of a cavity etched in a 1 mm thick silicon wafer with anodically bonded Pyrex windows. The measurement volume of the magnetometer is 1 mm^3, defined by the overlap region of a circularly polarized pump laser and a linearly polarized probe laser, both operated near 795 nm. Sensitivity limitations unique to the use of microfabricated cells are discussed.

©2010 Optical Society of America

OCIS codes: (020.0020) Atomic and molecular physics; (130.6010) Sensors.

References and links

1. D. Budker, and M. Romalis, "Optical magnetometry," Nat. Phys. **3**(4), 227–234 (2007).
2. I. K. Kominis, T. W. Kornack, J. C. Allred, and M. V. Romalis, "A subfemtotesla multichannel atomic magnetometer," Nature **422**(6932), 596–599 (2003).
3. H. B. Dang, A. C. Maloof, and M. V. Romalis, "Ultrahigh sensitivity magnetic field and magnetization measurements with an atomic magnetometer," Appl. Phys. Lett. **97**(15), 151110 (2010).
4. D. Drung, S. Bechstein, K. P. Franke, M. Scheiner, and T. Schurig, "Improved direct-coupled dc SQUID read-out electronics with automatic bias voltage tuning," IEEE Trans. Appl. Supercond. **11**(1), 880–883 (2001).
5. W. Happer, and H. Tang, "Spin-exchange shift and narrowing of magnetic resonance lines in optically pumped alkali vapors," Phys. Rev. Lett. **31**(5), 273–276 (1973).
6. J. C. Allred, R. N. Lyman, T. W. Kornack, and M. V. Romalis, "High-sensitivity atomic magnetometer unaffected by spin-exchange relaxation," Phys. Rev. Lett. **89**(13), 130801 (2002).
7. S. Knappe, V. Shah, P. D. D. Schwindt, L. Hollberg, J. Kitching, L. A. Liew, and J. Moreland, "A microfabricated atomic clock," Appl. Phys. Lett. **85**(9), 1460–1462 (2004).
8. M. P. Ledbetter, I. M. Savukov, D. Budker, V. Shah, S. Knappe, J. Kitching, D. J. Michalak, S. Xu, and A. Pines, "Zero-field remote detection of NMR with a microfabricated atomic magnetometer," Proc. Natl. Acad. Sci. U.S.A. **105**(7), 2286–2290 (2008).
9. K. Sternickel, and A. I. Braginski, "Biomagnetism using SQUIDs: status and perspectives," Supercond. Sci. Technol. **19**(3), S160–S171 (2006).
10. S. Knappe, T. H. Sander, O. Kosch, F. Wiekhorst, J. Kitching, and L. Trahms, "Cross-validation of microfabricated atomic magnetometers with superconducting quantum interference devices for biomagnetic applications," Appl. Phys. Lett. **97**(13), 133703 (2010).
11. V. Shah, S. Knappe, P. D. D. Schwindt, and J. Kitching, "Subpicotesla atomic magnetometry with a microfabricated vapour cell," Nat. Photonics **1**(11), 649–652 (2007).
12. J. Dupont-Roc, S. Haroche, and C. Cohen-Tannoudji, "Detection of very weak magnetic fields (10-9 gauss) by ^{87}Rb zero-field level crossing resonances," Phys. Lett. A **28**(9), 638–639 (1969).
13. W. C. Griffith, R. Jimenez-Martinez, V. Shah, S. Knappe, and J. Kitching, "Miniature atomic magnetometer integrated with flux concentrators," Appl. Phys. Lett. **94**(2), 023502 (2009).
14. S. K. Lee, and M. V. Romalis, "Calculation of magnetic field noise from high-permeability magnetic shields and conducting objects with simple geometry," J. Appl. Phys. **103**(8), 084904 (2008).
15. D. Robbes, "Highly sensitive magnetometers: a review," Sens. Actuators A Phys. **129**(1-2), 86–93 (2006).
16. G. Wallis, and D. I. Pomerantz, "Field assisted glass-metal sealing," J. Appl. Phys. **40**(10), 3946–3949 (1969).
17. S. Knappe, V. Gerginov, P. D. D. Schwindt, V. Shah, H. G. Robinson, L. Hollberg, and J. Kitching, "Atomic vapor cells for chip-scale atomic clocks with improved long-term frequency stability," Opt. Lett. **30**(18), 2351–2353 (2005).
18. T. W. Kornack, S. J. Smullin, S. K. Lee, and M. V. Romalis, "A low-noise ferrite magnetic shield," Appl. Phys. Lett. **90**(22), 223501 (2007).

19. M. P. Ledbetter, I. M. Savukov, V. M. Acosta, D. Budker, and M. V. Romalis, "Spin-exchange-relaxation-free magnetometry with Cs vapor," Phys. Rev. A **77**(3), 033408 (2008).
20. J. Preusser, V. Gerginov, S. Knappe, and J. Kitching, "A photonic atomic magnetometer," in preparation.

1. Introduction

Optically pumped alkali atom magnetometers [1] have recently reached sensitivities below one femtotesla in a 1 Hz bandwidth [2,3], comparable or better than those of the most sensitive low temperature superconducting quantum interference devices (SQUIDs) [4]. These ultra-high sensitivities have been achieved by operating at low magnetic fields and high alkali density, in a regime where spin-exchange collisions do not broaden the magnetic resonance [5,6]. Combining SERF magnetometry with microfabrication techniques first developed for chip-scale atomic clocks [7] could potentially lead to a low cost, mass-producible, non-cryogenic sensor with femtotesla sensitivity. Such a sensor could be used in applications such as remote detection of nuclear magnetic resonance (NMR) [8], and biomagnetic imaging [9,10].

The first SERF magnetometer based on a microfabricated vapor cell reached a magnetic sensitivity of $B_{sens} = 65$ fT/Hz$^{1/2}$ by use of a single light beam technique [11,12]. The addition of flux concentrators around the cell improved the sensitivity to 10 fT/Hz$^{1/2}$ [13], although this results in a much larger sensor volume with reduced spatial resolution. The sensitivity can also be improved by adding a second light beam in a perpendicular pump and probe configuration. This method resulted in a sensitivity of 20 fT/Hz$^{1/2}$ [11]. In this work we have improved our dual light beam SERF magnetometer sensitivity to 5 fT/Hz$^{1/2}$. The improved sensitivity was achieved by the addition of a counter-propagating optical pumping beam allowing operation at higher atomic densities, and the careful management of sources of thermal magnetic noise [14], especially from sources in the vapor cell itself, which are generally not as important an issue in a larger conventional glass cell. This result was achieved in a measurement volume of 1 mm^3, defined by the overlap region between the pump and probe light beams, giving an energy resolution per unit bandwidth [15] of $(B_{sens})^2 V / 2\mu_0 = 94\hbar$. This is within about a factor of two of the current best atomic magnetometer energy resolution per unit bandwidth of $44\hbar$, resulting from a sensitivity of 0.16 fT/Hz$^{1/2}$ obtained in a larger active volume of 0.45 cm^3 [3].

2. Experimental method

The vapor cells used in these measurements are fabricated from 1 mm thick silicon wafers. A cavity is etched into the wafer and then a Pyrex window is anodically bonded [16] to one side. ^{87}Rb atoms are deposited in the cavity by a process described in [17], along with 2 to 4 amg of N_2 buffer gas used to reduce the effects of wall depolarization and to collisionally quench excited-state ^{87}Rb atoms. The cell is then sealed by anodically bonding a second window to the wafer. Buffer gas densities up to 2 amg are achieved by backfilling the cell-filling chamber with N_2 gas at the desired density. In order to reach buffer gas densities higher than 2 amg, barium azide (BaN6) is added to the cell cavity before sealing, which then decomposes into Ba and N_2 gas when heat is applied to the cell.
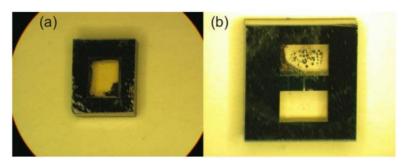
Fig. 1. Microfabricated vapor cells: (a) 3 mm x 2 mm x 1 mm single-chambered cell, (b) dual-chambered cell with two 3 mm x 2 mm x 1 mm cavities connected by a 1 mm x 0.1 mm passage.

Figure 1 shows a picture of two of the microfabricated vapor cells used in this work. Figure 1(a) shows a cell with a 3 mm x 2 mm chamber. The dark area in the corner of the cell is the remains of the reacted barium azide. In Fig. 1(b) there are two 3 mm x 2 mm chambers connected by a 1 mm x 0.1 mm passage. The second chamber allows magnetometry measurements to be made in a region isolated from the condensed Rb and Ba metals, so that the effects of Johnson noise [14] from these materials can be tested.
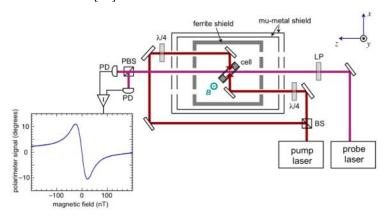

Fig. 2. Experimental setup. BS: beamsplitter, LP: linear polarizer, $\lambda/4$: quarter wave plate, PBS: polarizing beamsplitter, PD: silicon PIN photodiode.

Figure 2 shows an overview of the experimental setup. A microfabricated vapor cell is located in the middle of a three layer cylindrical magnetic shield. The two outer layers of shielding are 1.5 mm thick mu-metal, while the innermost is a 9 mm thick Mn-Zn ferrite layer [18] with inner dimensions of L = 10.2 cm and ID = 15.2 cm. The ferrite is used since it contributes less thermal magnetic noise than mu-metal, due to its lower electrical conductivity. Estimates of magnetic noise generated by the ferrite layer give 3 fT/$f^{1/2}$, or 0.3 fT/Hz$^{1/2}$ at 100 Hz. For comparison, a similarly sized 1.5 mm thick mu-metal layer would contribute thermal magnetic noise of about 10 fT/Hz$^{1/2}$.

The cell is heated to around 200 °C by passing current through two indium-tin-oxide (ITO) coated glass slides that surround the cell. The current through the heaters is turned on and off (50% duty cycle) with a period of 4 sec, and magnetic measurements are taken when the current is off. A circularly polarized pump beam tuned to the 795 nm D1 transition pumps the ^{87}Rb spins along the x-direction. A linearly polarized probe beam, detuned by 30 to 50 GHz from the D1 transition, is sent through the cell in the z-direction. Small magnetic fields in the y-direction are detected by monitoring the optical rotation of the probe beam with a balanced polarimeter. Typically, the pump beam power is 5 mW and the probe power is 200 µW.

Generally, sensitivity is improved by operating at higher temperatures and atomic densities, where higher signal levels can be achieved, but this improvement is eventually limited by the strong absorption of the pump/probe light in the optically thick vapor. The absorption of the probe light is mitigated by using polarization detection of a detuned probe beam. More efficient pumping of the optically thick vapor is achieved by splitting the pump beam into two beams of roughly equal intensity and opposite sense of circular polarization, which are directed through both the front and back of the cell. This helps to generate a more uniform polarization across the cell at high atomic densities. Comparatively, using a higher intensity single pump beam can also obtain high degrees of polarization, but gives a lower sensitivity due to power broadening of the magnetic resonance, especially at the front of the cell. The on resonance optical depth used in this work was typically in the range of 10 to 30.

3. Results and discussion

Magnetic sensitivity measurements were performed in three different microfabricated cells in this work: a 3 mm x 2 mm x 1 mm single-chambered cell, a 3 mm x 3 mm x 1 mm single-chambered cell, and the dual-chambered cell shown in Fig. 1(b). Figure 3 shows a magnetic noise spectrum obtained by use of the dual-chambered vapor cell. The two traces show the results from directing the light beams through the chamber where the Rb/Ba were initially deposited (green), and the other "clean" chamber (black). We generally find that $1/f$ type noise limits the sensitivity to around 70 Hz. This low-frequency noise may be attributable to light beam overlap jitter issues that might be alleviated by evacuating the beam paths, or by using optical fibers to reduce the free space light paths. We have previously found [11] that using a less sensitive single light beam technique without overlapping beams can give lower $1/f$ noise. At higher frequencies we find that the noise spectrum is relatively flat up to the ~200 Hz bandwidth of the magnetometer.
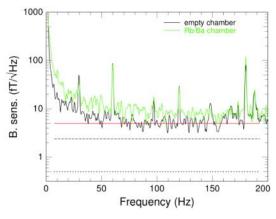

Fig. 3. Magnetic field sensitivity versus frequency in a dual-chambered microfabricated vapor cell. The red line indicates a sensitivity of 5 fT/Hz$^{1/2}$. The dashed line shows the estimated sensitivity limit due to photon shot noise, and the dotted line shows an estimate of the atom (spin-projection) noise based on App. A in Ref. [19].

In the case of the dual-chambered cell, the sensitivity reaches 5 fT/Hz$^{1/2}$ in the "empty" chamber, while the Rb/Ba chamber is limited to 8 fT/Hz$^{1/2}$. For the single-chambered cells we found that the 3 mm x 2 mm x 1 mm cell was limited to 10 fT/Hz$^{1/2}$, and the 3 mm x 3 mm x 1 mm cell was limited to 8 fT/Hz$^{1/2}$ magnetic sensitivity. These sensitivity limits seemed to be intrinsic to the cells, and were repeatable under a variety of cell temperatures and light beam conditions.

Table 1 shows possible magnetic thermal noise contributions from materials near the vapor cell, as calculated by the methods described in [14]. Contributions from condensed Rb are potentially very significant, depending on the details of the distribution of Rb droplets, or the thickness of a Rb film. The cells visibly contain ~100 μm droplets that could easily lead to

magnetic Johnson noise at the observed level in the single-chambered cells. This noise is avoided by using a Rb reservoir, such as the dual-chambered cells used in this work, allowing the magnetometer measurements to be made at a greater separation from the condensed Rb. In this case, the performance is improved from 8 fT/Hz$^{1/2}$ to 5 fT/Hz$^{1/2}$ by including a Rb reservoir. Proper thermal management must be maintained so that the reservoir is the coldest part of the cell.

Table 1. Limits on magnetic sensitivity due to thermal magnetic noise in nearby materials

Source	Resistivity ($\Omega \cdot$cm)	Approx. distance (mm)	Noise (fT/Hz$^{1/2}$)
Silicon (CZ)	5	1	3
Silicon (FZ)	8000	1	0.01
Rb film (1 nm thick)	1.3×10^{-5}	0.5	3
Rb sphere (100 μm diam.)	1.3×10^{-5}	0.5	7
ITO film	$\rho/t = 50\ \Omega$ [a]	1	3
Heater connections	< 0.001	12	2
Cu wire (0.32 mm diam.)	1.7×10^{-6}	30	< 0.1
Mirrors	1.6×10^{-6}	50	0.14
Ferrite shield	500	75	0.3 (@ 100 Hz)

[a] The ITO resistivity (ρ) is not known for the heaters used in this work, but the measured value of ρ/t, where t is the film thickness, is what is required to calculate the thermal magnetic noise from a thin film [14].

The silicon cell body is another potential source of Johnson noise in these types of cells. The single-chambered cell used in this work was fabricated from Czochralski (CZ) method grown silicon with conductivity in the range 1 to 20 $\Omega \cdot$cm. As shown in Tab. 1, cells using this type of silicon would be limited to a few fT/Hz$^{1/2}$ by Johnson noise. CZ type silicon is available with up to 100 Ω cm resistivity, but to obtain higher resistivities, higher purity silicon grown with the Float Zone (FZ) method must be used. The dual-chambered cell used in this work was fabricated from FZ silicon with a resistivity of 8000 $\Omega \cdot$cm, which should avoid Johnson noise down to a level of 0.01 fT/Hz$^{1/2}$.

Possibly the sensitivity results with the dual-chambered cell are next limited by Johnson noise from the ITO cell heaters (the ITO film, and electrically conductive heater connections) used in this work. There is potential for further improvement if we remove these conductive elements and switch to a different heating method, such as optical heating [20], forced heated airflow, or an electrically heated oven with the electrically conductive elements moved further away from the cell.

4. Summary

We have demonstrated an atomic magnetometer with 5 fT/Hz$^{1/2}$ sensitivity in a dual-chambered, microfabricated vapor cell. This result corresponds to an energy resolution per unit bandwidth of 94 $\hbar$, within a factor of two of the best result in an atomic magnetometer.

Achieving this sensitivity level requires careful management of Johnson noise sources in the vapor cell, such as the distribution of condensed alkali metal on the cell walls. This issue is mitigated in conventional glass-blown cells typically used in atomic magnetometers, where the larger cell dimensions guarantee a larger separation between the measurement region and the cell walls. Reaching the femtotesla regime in microfabricated cells also requires the use of very high purity, high resistivity FZ silicon for the cell body. This type of sensor can potentially be used as a non-cryogenic alternative to SQUID sensors in some applications.

Acknowledgements